Deep ocean ^{14}C ventilation age reconstructions from the Arctic Mediterranean reassessed

Mohamed M. Ezat [a,b,c,*], Tine L. Rasmussen [a], Luke C. Skinner [b], Katarzyna Zamelczyk [a]

[a] CAGE – Centre for Arctic Gas Hydrate, Environment and Climate, Department of Geosciences, UiT, The Arctic University of Norway, Norway
[b] Godwin Laboratory for Palaeoclimate Research, Department of Earth Sciences, University of Cambridge, UK
[c] Department of Geology, Faculty of Science, Beni-Suef University, Beni-Suef, Egypt

ABSTRACT

The present-day ocean ventilation in the Arctic Mediterranean (Nordic Seas and Arctic Ocean), via transformation of northward inflowing warm Atlantic surface water into cold deep water, affects regional climate, atmospheric circulation and carbon storage in the deep ocean. Here we study the glacial evolution of the Arctic Mediterranean circulation and its influence on glacial climate using radiocarbon reservoir-age reconstructions on deep-sea cores from the Fram Strait that cover the late glacial period (33,000–20,000 yr ago; 33–20 ka). Our results show high Benthic-Planktic ^{14}C age differences of ∼1500 ^{14}C years 33–26.5 ka suggesting significant water column stratification between ∼100–2600 m water depth, and reduction and/or shoaling of deep-water formation. This phase was followed by break-up of the stratification during the Last Glacial Maximum (LGM; 26–20 ka), with Benthic-Planktic ^{14}C age differences of ∼250 ^{14}C years, likely due to enhanced upwelling. These ocean circulation changes potentially contributed to the final intensification phase of glaciation via positive cryosphere-atmosphere-ocean circulation-carbon cycle feedbacks. Our data also do not support 'extreme aging' of >6000 ^{14}C years in the deep Arctic Mediterranean, and appear to rule out the proposed outflow of very old Arctic Ocean water to the Nordic Seas during the LGM and to the subpolar North Atlantic Ocean during the deglacial period.

© 2019 The Authors. Published by Elsevier B.V. This is an open access article under the CC BY-NC-ND license (http://creativecommons.org/licenses/by-nc-nd/4.0/).

1. Introduction

The Atlantic Meridional Overturning Circulation (AMOC) plays a key role in the Earth's climate system through its control on heat, freshwater, nutrient and greenhouse gas transports (Ganachaud and Wunsch, 2000; Rahmstorf, 2000; Takahashi et al., 2009). At present, the northern limb of the AMOC constitutes water mass transformation of northward inflowing warm Atlantic surface water to cold deep water through local overturning. This well-ventilated deep water in the Arctic Mediterranean has a ventilation age of ∼500 yr, which is close to the surface water reservoir age of ∼400 yr (e.g., Hansen and Østerhus, 2000; Broecker and Peng, 1982; Mangerud et al., 2006). The well-ventilated deep water overflows the Greenland-Scotland Ridge into the North Atlantic Ocean, forming a major part of the lower North Atlantic Deep Water (NADW) (e.g., Hansen and Østerhus, 2000).

Paleoclimate research seeks a better understanding of AMOC-climate interactions through the study of the behavior of the AMOC and its controlling mechanisms under different climate states and on different time scales (e.g., Clark et al., 2002; Skinner et al., 2014; Pena and Goldstein, 2014). In this regard, the structure and vigor of the AMOC during the Last Glacial Maximum (LGM; 26–19 ka, e.g., Clark et al., 2009) have been intensively investigated (e.g., Sarnthein et al., 1994; Curry and Oppo, 2005; Otto-Bliesner et al., 2007; Keigwin and Swift, 2017). However, several aspects of the AMOC operation during the LGM remain largely unconstrained. For example, contrasting scenarios of deep ocean circulation in the Arctic Mediterranean during the LGM have been proposed, ranging from near-cessation to vigorous, as present-day, ocean ventilation (e.g., Veum et al., 1992; Bauch et al., 2001; Hoffmann et al., 2013; Thornalley et al., 2015; Meinhardt et al., 2016). Many paleoceanographic studies of this issue are based on radiocarbon dating of marine carbonates (e.g., foraminifera, corals and mollusks) to infer past changes in ocean ventilation, based on the premise that these marine carbonates record the radiocarbon activity of ambient seawater (e.g., Broecker et al., 2004; Adkins and Boyle, 1997). Radiocarbon age offsets between con-
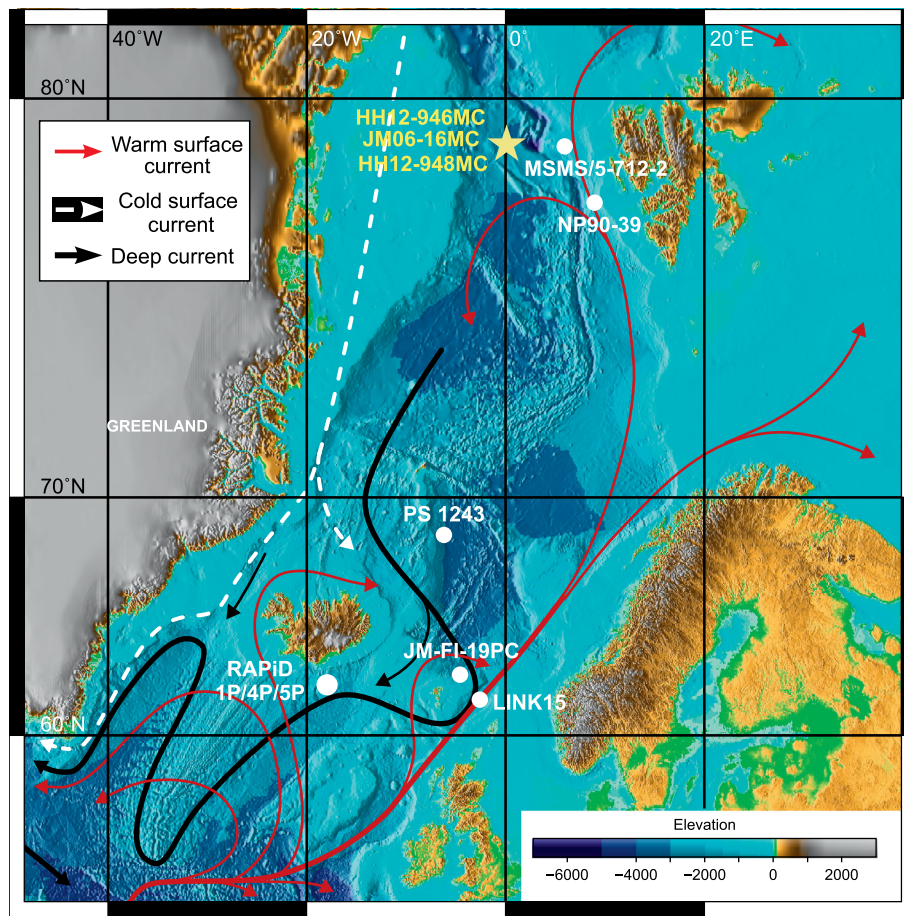

Fig. 1. Major surface and deep-water currents in the Nordic Seas (e.g., Hansen and Østerhus, 2000) and sediment core locations. Yellow star refers to location of investigated sediment cores HH12-946MC and HH12-948MC (this study) and sediment core JM06-16MC published by Zamelczyk et al. (2012). White circles refer to other core sites discussed in the text. Map is modified from Ezat et al. (2014, 2017). (For interpretation of the colors in the figure(s), the reader is referred to the web version of this article.)

temporary benthic (B) and planktic (P) foraminifera (B-P age differences) have been used as a proxy for ocean mixing between (near)surface and bottom waters (e.g., Broecker et al., 2004). This ventilation proxy is best applied in regions where localized deep mixing exerts a significant influence on local deep-water radiocarbon activity. When independent calendar ages for marine records or knowledge about past surface reservoir ages are available, B-P age differences can be converted into Benthic-Atmosphere (here referred to as B-A) age differences. This allows for deep-ocean radiocarbon activities from contrasting hydrographic regimes to be correlated to a common atmospheric reference and provide a measure of the local deep ocean-atmosphere radiocarbon isotope disequilibrium (e.g., Skinner et al., 2010; for details about different methods for reconstructing ^{14}C-ventilation ages see Cook and Keigwin, 2015).

Benthic-atmosphere ^{14}C ventilation reconstructions from 2711 m water depth in the northern Norwegian Sea have been employed to suggest an extreme aging (up to 10,000 ^{14}C years) and near-isolation of the deep Arctic Mediterranean during the LGM (Thornalley et al., 2015). Episodic overflows of this aged Arctic/Nordic Seas reservoir into the subpolar North Atlantic across the Greenland-Scotland Ridge may have occurred during the last deglaciation (Thornalley et al., 2011, 2015; Ezat et al., 2017). However, this scenario is inconsistent with reconstructions based on Nd isotope and Pa/Th proxies that suggest vigorous ocean circulation in the Arctic Ocean during the late glacial period (Hoffmann et al., 2013; Meinhardt et al., 2016).

In this study, we investigate ventilation and ocean circulation changes in the central Fram Strait leading to and during the LGM

related to climate variability using ^{14}C dates on benthic and planktic foraminiferal species. Thornalley et al. (2015) suggested that the inferred extremely aged water in the deep Norwegian Sea during the LGM was sourced from the central Arctic Ocean. The Fram Strait, the only deep gateway for exchange of deep water between the Arctic Ocean and the Nordic Seas, must therefore record the signature of this hypothesized Arctic outflow to the Nordic Seas. This makes the Fram Strait an ideal location to test the hypothesis of existence of an Arctic deep-water endmember with a ventilation age >6000 yr and its subsequent inflow to the Nordic Seas during the LGM.

2. Materials and methods

Two deep-sea multicores HH12-946MC (78°53′N; 01°45′W; 2637 m water depth, 42 cm length) and HH12-948MC (78°52′N; 00°21′E; 2542 m water depth, 44.5 cm length) were retrieved from the central Fram Strait during a cruise with R/V Helmer Hanssen in July 2012 (Fig. 1). The two sediment cores have been sampled at 0.5 cm intervals on-board. The samples were weighed and freeze-dried. Subsequently, the dry samples were weighed and wet sieved through 1000, 500, 100 and 63 μm mesh-sizes. The residues were dried and weighed. More than 300 benthic foraminiferal specimens in core HH12-946MC from the size fraction >100 μm were counted and identified to species level. The number of benthic foraminifera in the deglacial part of the record was too low for quantification.

For stable carbon and oxygen isotope analyses ~30 specimens of the planktic foraminiferal species *Neogloboquadrina pachyderma*

Table 1
Benthic and planktic ^{14}C data from sediment core HH12-946MC. The δ^{13}C was measured by a gas source mass spectrometer. Benthic ^{14}C-dates from top centimeter of the core yielded too young ages and are not plotted in Fig. 4. Abbreviations: *Neogloboquadrina pachyderma* (*N. p*), *Oridorsalis umbonatus* (*O. u*), *Pyrgo depressa* (*P. d*), Benthic-planktic ^{14}C age offset (B-P offset), Marine Isotope Stage (MIS). Asterisks refer to ^{14}C dates graphitized at the ^{14}Chrono Centre, Queen's University Belfast, whereas all other ^{14}C dates were graphitized at the University of Cambridge. All radiocarbon dates were analyzed at the ^{14}Chrono Centre, Queen's University Belfast.

Time interval	Depth (cm)	Calendar age (ka)	Species	^{14}C age (yr)	Error (yr)	B-P offset (yr)	δ^{13}C (‰)
Mid	1.25	4.9	*N. p*	4667	28		0.06
Holocene	1.25	4.9	*O. u*	2884	30	−1783	−0.42
	1.25	4.9	*P. d*	1362	28	−3305	−0.43
	1.25	4.9	*P. d*	1297	28	−3370	
	3.75	6.0	*N. p*	5620*	30		−0.01
	3.75	6.0	*O. u*	5835*	30	215	−0.8
Early	24	21.0	*O. u*	18335	80	367	−1.7
MIS 2	24.25	21.2	*N. p*	17968	80		−0.78
	25.25	21.4	*N. p*	18280*	75		−0.64
	25.25	21.4	*N. p*	18075	90		
	25.25	21.4	*O. u*	18580	88	505	−1.9
	25.75	21.8	*N. p*	18399	75		
	25.75	21.8	*O. u*	18511	82	112	−1.83
	27.25	22.3	*N. p*	18765	73		−0.64
	27.25	22.3	*O. u*	18787	95	22	−1.92
	28.25	22.8	*N. p*	19335	77		−0.58
	28.25	22.8	*O. u*	19232	148	−103	−1.86
Late	30.75	26.1	*N. p*	22372	108		−0.88
MIS 3	30.75	26.1	*P. d*	32400	329	10028	1.04
	31.25	26.4	*P. d*	33434*	459	10711	0.72
	32.75	27.1	*N. p*	23016*	140		−0.61
	32.75	27.1	*N. p*	23076	131		
	32.75	27.1	*O. u*	25327	161	2251	−1.49
	32.75	27.1	*P. d*	31975	312	8899	0.71
	33.75	28.4	*N. p*	24741	134		−0.83
	33.75	28.4	*O. u*	26118	170	1377	−1.35
	34.75	30.0	*P. d*	38639*	832	12102	
	35.75	31.6	*N. p*	28333	225		−0.37
	35.75	31.6	*O. u*	29715	340	1382	−1.21
	37.25	33.4	*N. p*	29497*	274		−0.41
	37.25	33.4	*P. d*	40749*	1075	11252	1.1

(size fraction 125–150 μm), ∼20 specimens of the shallow infaunal benthic foraminifera *Oridorsalis umbonatus* (size fraction 150–250 μm), ∼5 specimens of the epifaunal benthic foraminifera *Cibicidoides wuellerstorfi* (size fraction 250–500 μm) and 1 specimen of the infaunal benthic foraminifera *Pyrgo depressa* (size fraction 500–1000 μm) were picked. The planktic stable isotopes were measured at Leibniz Laboratory for Radiometric Dating and Stable Isotope Research in Kiel, Germany, while the benthic (*O. umbonatus* and *C. wuellerstorfi*) stable isotopes were measured at the Godwin Laboratory for Paleoclimate Research, University of Cambridge, UK for sediment core HH12-946MC and at UiT, the Arctic University of Norway for sediment core HH12-948MC. Stable isotope measurements in *P. depressa* were performed at UiT, the Arctic University of Norway. Many studies account for the vital effects (deviation of foraminiferal δ^{18}O from 'equilibrium' values) using species-specific corrections (e.g., Bauch et al., 2001). In this study, we did not apply any corrections because we only discuss relative changes in δ^{18}O records (in particular δ^{18}O differences between *N. pachyderma* and *O. umbonatus*), which are not affected by corrections. In addition, corrections for *N. pachyderma* vary from 0.0 to −1.6‰ in different studies (see e.g., Pados et al., 2015).

We picked samples of *O. umbonatus* (size fraction 150–250 μm; 2 to 3 mg carbonate), *N. pachyderma* (size fraction 250–500 μm; 3 to 5 mg carbonate) and where available, mixed species of genus *Pyrgo* (mainly *Pyrgo depressa*; size fraction >500 μm) from sediment core HH12-946MC for radiocarbon dating. All specimens were carefully inspected under the microscope in order to inspect for any signs of contamination and only pristine specimens were included in the analyses. Foraminiferal samples were graphitized at the University of Cambridge (see Freeman et al., 2015

for detailed methodology) and subsequently analyzed by accelerator mass spectrometry at the ^{14}Chrono Centre, Queen's University Belfast, Northern Ireland. Some additional samples were both graphitized and analyzed at the ^{14}Chrono Centre, Queen's University Belfast (Table 1), and two new samples (*Pyrgo rotalaria* and *N. pachyderma*) from sediment core LINK15 (61°45′N; 2°40′W, 1602 m water depth; Olsen et al., 2014) were also graphitized and analyzed there. No pretreatment was applied for the samples graphitized at the University of Cambridge, whereas samples graphitized at the Queen's University of Belfast were cleaned prior to the graphitization using 2 ml 15% hydrogen peroxide (with ultra-sonication for 3 min). Samples with and without pretreatment yielded indistinguishable results (Table 1). We also crushed the specimens of *Pyrgo* to check the inside of the shells for presence of diagenetic carbonate fillings inside different chambers as in Keigwin (1979). All specimens analyzed were pristine also on the inside of the shells.

2.1. Age models

We constructed the age models of sediment cores HH12-946MC and HH12-948MC based on twelve and four calibrated planktic foraminiferal ^{14}C dates, respectively (Fig. 2). The planktic radiocarbon dates were calibrated using the Calib7.04 program and the Marine13 calibration dataset (Reimer et al., 2013). We implemented the reservoir age correction of 405 yr inherent in the Calib program (Stuiver and Reimer, 1993), which is close to modern reservoir age of the surface ocean in the open Nordic Seas of ∼400 yr (e.g., Mangerud et al., 2006). The surface reservoir ages varied during the glacial period due to changes in ocean circulation and
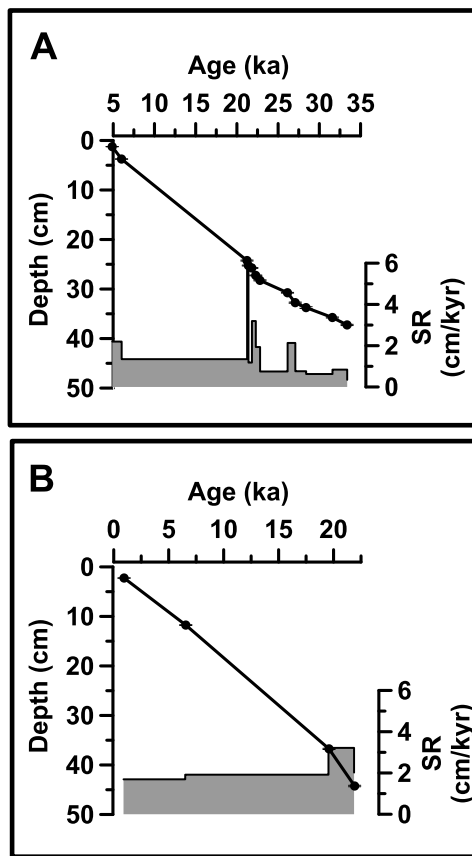
Fig. 2. Age models for sediment cores HH12-946MC (A) and HH12-948MC (B) based on calibrated ^{14}C dates measured in planktic foraminiferal species *Neogloboquadrina pachyderma*. Sedimentation rates are shown at the bottom of the figure panels. Error bars associated with radiocarbon dates represent one standard deviation.
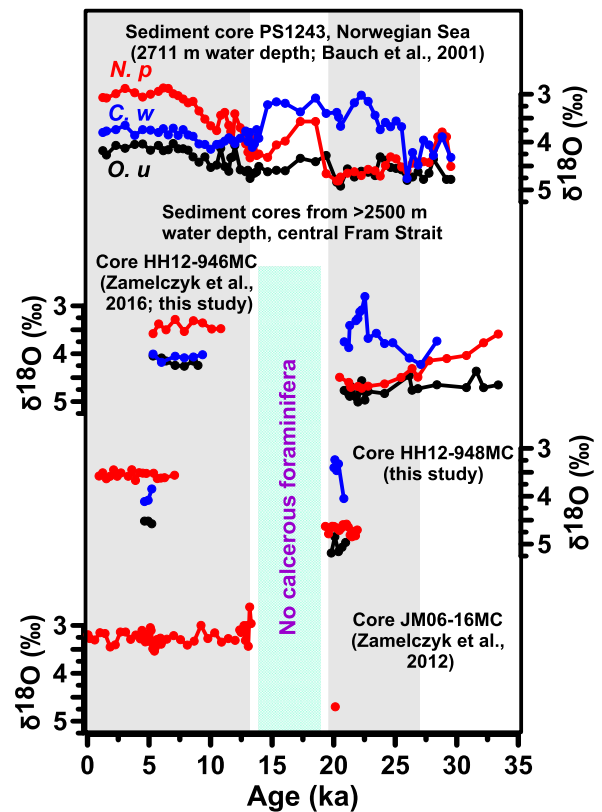

Fig. 3. Oxygen isotope records from the Fram Strait and the central Nordic Seas. Foraminiferal species used are *Neogloboquadrina pachyderma* (*N. p*; red), *Oridorsalis umbonatus* (*O. u*; black) and *Cibicidoides wuellerstorfi* (*C. w*; blue).

carbon cycle (e.g., Bard, 1988). We lack information about temporal changes in reservoir ages at the central Fram Strait during the last glacial. However, we discuss in detail the effects of past changes in reservoir ages on our results as well as on the age models (see Discussion). Following the same approach, we re-calibrated previously published planktic ^{14}C dates from sediment cores MSM5/5-712-2 (78°55′N; 6°46′E; 1487 m water depth; Zamelczyk et al., 2014; Müller and Stein, 2014), JM06-16MC (78°54′N; 01°69′E, 2546 m water depth; Zamelczyk et al., 2012), NP90-39 (77°16′N; 09°06′E, 2119 m water depth; Hebbeln et al., 1994; Dokken and Hald, 1996) and PS1243 (69°37′N; 06°55′W, 2711 m water depth; Bauch et al., 2001; Thornalley et al., 2015). Accordingly, the age models were re-calculated to obtain comparable time-scales with our sediment cores HH12-946MC and HH12-948MC ignoring possible, but probably small, spatial variabilities in reservoir ages at a given time for these nearby core sites. The originally published age models for the time intervals of interest in this study (see section 2.2) are based on planktic foraminiferal ^{14}C dates except for core PS1243, which is based on alignment of marine planktic foraminiferal δ^{18}O and Greenland ice core δ^{18}O (Thornalley et al., 2015). Thus, the modification to these age models, except for core PS1243, only includes the use of the radiocarbon calibration of Reimer et al. (2013) instead of using no (e.g., Hebbeln et al., 1994) or other calibration curves (e.g., Müller and Stein, 2014). We also discuss the potential impact of using the age model from Thornalley et al. (2015) (see Supplementary Fig. 2). The sedimentation rates in both cores range from 1 to 3 cm/kyr, except for the interval 19.7–19.5 ka in core HH12-946MC, where the calculated sedimentation is 6 cm/kyr (Fig. 2). Thus, a 0.5 cm sample spans ∼300–500 yr, which potentially can induce a large error on ^{14}C dates (e.g., Peng and Broecker,

1984). However, because the distribution patterns of the benthic foraminiferal species *O. umbonatus*, *C. wuellerstorfi* and *Pyrgo* spp. show some abrupt changes (Supplementary Fig. 1) and because the ^{14}C dates of *N. pachyderma* and *O. umbonatus* are in chronological order (Table 1), we assume the error is insignificant.

2.2. Selection of sediment cores, foraminiferal species and time-slices

The δ^{18}O records of three sediment cores from the central Fram Strait (Zamelczyk et al., 2012, 2016 and this study) and one sediment core from the central Nordic Seas (Bauch et al., 2001) are compared (Fig. 3). All planktic, epifaunal and infaunal benthic δ^{18}O records from both areas display the same glacial to interglacial variability (Fig. 3). Bauch et al. (2001) observed that the δ^{18}O measured in the epifaunal benthic species *C. wuellerstorfi* from the LGM sediments in the northern Norwegian Sea are lower compared to the Holocene in contrast to the infaunal benthic δ^{18}O records. The same feature is found in the two sediment cores from the central Fram Strait with average LGM δ^{18}O of ∼3.4‰ and ∼4.8‰ for *C. wuellerstorfi* and *O. umbonatus*, respectively, whereas both species show similar Holocene δ^{18}O of ∼4.1‰ (Fig. 3). At 2781 m water depth in the southern Norwegian Sea (Veum et al., 1992) both *C. wuellerstorfi* and *O. umbonatus* show the same LGM δ^{18}O (=∼4.8‰) as recorded in our records by *O. umbonatus* (Fig. 3). The 'peculiar' low LGM δ^{18}O in *C. wuellerstorfi* is therefore restricted to the deep central and northern Nordic Seas (Bauch et al., 2001; this study). Deep-sea records from the central Arctic Ocean do not contain LGM sediments (e.g., Hanslik et al., 2010) and thus we are not able to trace the northern extent of the low *C. wuellerstorfi* δ^{18}O. The relative abundance of *C. wuellerstorfi* in the LGM sediment is very low (Supplementary Fig. 1) with only ∼7 specimens per sample on average. Low δ^{18}O in *C. wuellerstorfi* has been explained by influence of an ephemeral water mass

with very low $\delta^{18}O$, though the possibility of unknown *C. wuellerstorfi*-specific 'vital effects' occurring under LGM conditions cannot be excluded (Bauch et al., 2001). We are not able to assess these different explanations and we suggest that future work take advantage of recently developed radiocarbon analytical techniques that are capable of dating a few hundreds of micrograms of carbonate (e.g., Gottschalk et al., 2018) to ensure that these *C. wuellerstorfi* with low $\delta^{18}O$ are of LGM age and not transported specimens or reworked. We emphasize that the 'peculiar' low LGM $\delta^{18}O$ of *C. wuellerstorfi* are consistent between records in the central and northern Nordic Seas (Fig. 3), which merits further investigation.

Similar to the central Nordic Seas (Bauch et al., 2001), our records show that the benthic foraminiferal assemblages from the deep Fram Strait are dominated almost exclusively by *O. umbonatus* during the LGM (Supplementary Fig. 1). We therefore focus the discussion on *O. umbonatus* as this species is most likely to record the average long-term bottom water conditions during the LGM in the deep Fram Strait and the northern/central Nordic Seas (see also Bauch et al., 2001).

We mainly base the reconstruction of the past ocean ventilation in the Fram Strait on sediment core HH12-946MC, because it is the longest record (spanning the past ∼40 kyr) of our three sediment cores. In this study, we focus on the past 33 kyr. The sediments dating from the deglaciation >2500 m water depth from the Fram strait in both cores HH12-946MC and HH12-948MC contain only a few calcareous and agglutinated foraminifera or are completely barren (Fig. 3). This was also found by Zamelczyk et al. (2012) in nearby core JM06-16MC (Fig. 3). Whether the absence of foraminifera resulted from unfavorable environmental conditions, such as extremely high salinity, low oxygen or low food supply, or from post-mortem dissolution requires further investigation. However, we note that this feature has not been recorded from other deep areas (>2500 m water depth) further south in the Nordic Seas (e.g., Bauch et al., 2001; Thornalley et al., 2015), or from shallower areas in the Fram Strait (Bauch et al., 2001). In deep-sea records from the central Arctic Ocean, sediments from the late deglaciation (∼13.5–10 ka) also contain calcareous foraminifera (e.g., Hanslik et al., 2010). Thus, it seems that this feature was restricted to the deep central Fram Strait. Future work focusing on biomarkers and sediment provenance may help to clarify the origin of this largely carbonate/foraminifera free sediment interval. In this study, we therefore focus on three time slices: late Marine Isotope Stage 3 (MIS 3) (33–26 ka), LGM (26–20 ka) and early/mid Holocene (10–5 ka).

3. Results and discussion

3.1. Ocean circulation changes in the Fram Strait leading to and during the LGM

The ^{14}C age differences between the co-existing benthic foraminiferal species *O. umbonatus* and the planktic species *N. pachyderma* (B_{Ou}-P_{Np} age difference) range from ∼2200 to 1400 ^{14}C years during late MIS 3 (∼33–26.5 ka) (Fig. 4e). These B_{Ou}-P_{Np} age differences are an order of magnitude higher than the modern deep to surface water ^{14}C age difference in the region (∼100 yr) indicating a strong stratification of the water column during late MIS 3 and pointing to reduced deep water formation in the Nordic Seas. However, presence of an active, but shallower convection cell cannot be ruled out. The absence of independent constraints on the calendar age chronology and surface reservoir age offsets prevents an exact estimate of the ventilation age of the deep water (i.e., B-A ^{14}C ventilation age). If near-surface reservoir age estimates from the central Nordic Seas (∼400–650 yr; Thornalley et al., 2015; see Fig. 4d) are assumed to apply, the B-A age difference in the deep Fram Strait would have been ∼2000 ^{14}C years
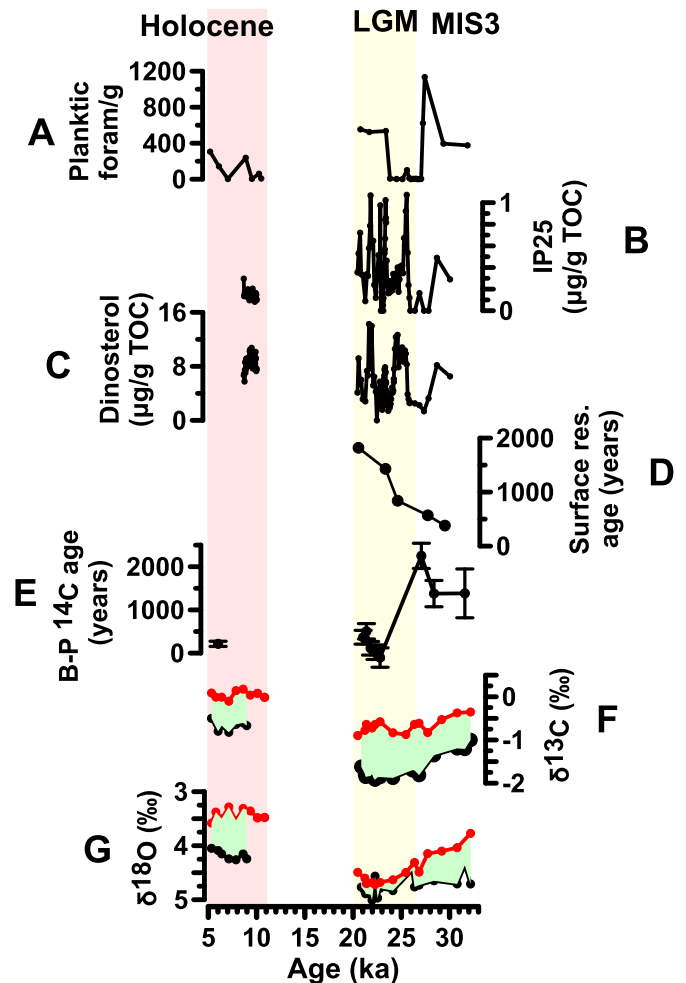

Fig. 4. Ocean circulation and primary productivity reconstructions from the Fram Strait. (A) Concentration of planktic foraminifera from sediment core NP90-39 (Hebbeln et al., 1994). **(B)** C25 isoprenoid lipid (IP$_{25}$) from sediment core MSM5/5-712-2 (Müller and Stein, 2014). High concentration of IP25 suggests presence of seasonal sea ice, whereas absence of IP25 suggests either permanent sea-ice cover (when the concentration of phytoplankton-induced sterols is low) or open ocean conditions (when the concentration of phytoplankton-induced sterols is high) (see Müller and Stein, 2014 for details). **(C)** Concentration of dinosterol from sediment core MSM5/5-712-2 (Müller and Stein, 2014). **(D)** Near-surface reservoir ages from sediment core PS1243 (Bauch et al., 2001; Thornalley et al., 2015; see Supplementary Fig. 2). **(E)** Benthic-Planktic ^{14}C age difference from sediment core HH12-946MC. Error bars are combined 1σ errors in planktic and benthic ^{14}C dates. **(F)** $\delta^{13}C$ measured in *Oridorsalis umbonatus* (black) and *Neogloboquadrina pachyderma* (red) from sediment core HH12-946MC. **(G)** $\delta^{18}O$ measured in *Oridorsalis umbonatus* (black) and *Neogloboquadrina pachyderma* (red) from sediment core HH12-946MC (Zamelczyk et al., 2016 and this study).

during late MIS 3. These B-A age difference estimates should be taken with a great caution, because of the large distance between the two areas (Fig. 1) and the large uncertainties associated with the surface reservoir ages in Thornalley et al. (2015). It has been suggested that surface advection of Atlantic water to the eastern Fram Strait took place during late MIS 3 based on high abundance of planktic foraminifera (Hebbeln et al., 1994; Dokken and Hald, 1996; see Fig. 4a). Studies based on phytoplankton-produced sterols and C25 isoprenoid lipid (IP25) from the eastern Fram Strait however, suggest that perennial sea ice conditions generally predominated in the period ∼30–26.5 ka (e.g., Müller and Stein, 2014; see Fig. 4b, c). It is therefore possible that the Fram Strait during late MIS 3 was similar to the Arctic Ocean today, where the sea ice cover is insulated from subsurface Atlantic water by a cold halocline (e.g., Aagaard et al., 1985), but with significantly reduced deep-water formation.

At the transition from MIS 3 to LGM at ~26 ka, all proxy records show distinct changes (Fig. 4). The average B_{Ou}-P_{Np} age difference decreases from ~1500 ^{14}C years in late MIS 3 (32–26.5 ka) to ~250 ^{14}C years during the late LGM (23–20 ka) (Fig. 4e). This is associated with an increase in the difference between *N. pachyderma* $\delta^{13}C$ and *O umbonatus* $\delta^{13}C$ (P_{Np}-B_{Ou} $\delta^{13}C$) and a decrease in the difference between *O. umbonatus* $\delta^{18}O$ and *N. pachyderma* $\delta^{18}O$ (B_{Ou}-P_{Np} $\delta^{18}O$) (Fig. 4f, g); indicative of the biological and physical state in the Fram Strait during the LGM. We interpret the decrease in B_{Ou}-P_{Np} age difference and the decrease in B_{Ou}-P_{Np} $\delta^{18}O$ as reduction in stratification and a more homogeneous water column. The increase in P_{Np}-B_{Ou} $\delta^{13}C$ is indicative of presence of an enhanced nutrient gradient in the water column (cf., Kroopnick, 1985) and points to increase in primary productivity. The increase in the concentration of phytoplankton-produced sterols, though highly variable, in the eastern Fram Strait during the LGM relative to late MIS 3 supports the suggested increase in primary productivity during the LGM (Müller and Stein, 2014; Fig. 4c). Together, the observed changes likely indicate upwelling of nutrient-rich water.

If the water column de-stratification during the LGM (evident from the decrease B_{Ou}-P_{Np} ^{14}C age difference) was achieved via downwelling (e.g., open ocean convection or brine formation), the decrease in the B_{Ou}-P_{Np} $\delta^{18}O$ would have been caused mainly by a change in benthic $\delta^{18}O$ (i.e., transfer of surface water signal to deep water) rather than a change in planktic $\delta^{18}O$ (i.e., transfer of deep water signal to surface water). At the transition from late MIS3 to the LGM, *O. umbonatus* $\delta^{18}O$ remain almost constant, whilst *N. pachyderma* $\delta^{18}O$ increase by ~0.4‰ (Fig. 4g). During the LGM, both *N. pachyderma* and *O. umbonatus* $\delta^{18}O$ increased by ~0.2‰. If some of the change in B_{Ou}-P_{Np} $\delta^{18}O$ is due to changes in local seawater $\delta^{18}O$, a part of the increase in *N. pachyderma* $\delta^{18}O$ from MIS 3 to the LGM is likely due to mixing with upwelled deep water with higher $\delta^{18}O$. The ~0.2‰ increase in both *N. pachyderma* and *O. umbonatus* $\delta^{18}O$ during the LGM may have been caused by the continuing growth of the LGM ice sheets until 21 ka (e.g., Hughes et al., 2016). Possible changes in the surface-deep water temperature and/or salinity gradient may have caused/contributed to the observed changes in B_{Ou}-P_{Np} $\delta^{18}O$ difference from late MIS3 to LGM, which represents a source of uncertainty in our interpretations of B_{Ou}-P_{Np} $\delta^{18}O$ difference changes.

Thornalley et al. (2015) observed an increase in near-surface reservoir ages in the central Nordic Seas from ~450 ^{14}C years in late MIS 3 to ~1400 ^{14}C years during the LGM (Fig. 4d). Upwelling of deep aged water could have caused this increase in the near-surface reservoir age. If this is correct, it would imply that the decrease in the B_{Ou}-P_{Np} age difference resulted from an increase in the near-surface reservoir age and aging of the entire water column, rather than from a decrease in the deep water reservoir age. Taking these near-surface reservoir ages into account, the ventilation age of deep water in the Fram Strait may have remained around 2000 ^{14}C years during the late MIS 3 and the LGM, though the water column mixing processes and dynamics were very different during these two time periods. We acknowledge the large uncertainty in our estimates for LGM deep water reservoir ages given the poor control on the calendar age chronology in our records, and the large uncertainties associated with the surface reservoir age estimates in Thornalley et al. (2015). Nevertheless, these estimates are consistent with deep-ocean reservoir-age reconstructions from the southern Norwegian Sea and the North Atlantic for the LGM (Ezat et al., 2017; Skinner et al., 2014).

3.2. Reassessment of Arctic Mediterranean ventilation age reconstructions

Our result from the Fram Strait has significant implications for previous ^{14}C ventilation-age reconstructions from the Arctic Mediterranean and the subpolar North Atlantic. As mentioned above, Thornalley et al. (2015) published data that indicated that Arctic Mediterranean deep water aged by up to >10,000 ^{14}C years during the LGM. A later study by Ezat et al. (2017) based on sediment cores from ~1200 m water depth from the southern Norwegian Sea and the Iceland Basin showed that radiocarbon dates measured in *Pyrgo* and other miliolids apparently confirmed old ages of deep-water overflows of >6000 yr from the Arctic Mediterranean to the subpolar North Atlantic during the last deglaciation. However, radiocarbon dating of other benthic foraminiferal species from the same sample set yielded ventilation ages <2500 ^{14}C years (Ezat et al., 2017). Two scenarios for the interspecies benthic foraminiferal ^{14}C age offsets were proposed. First, different benthic foraminiferal species dated from the same sample that may span tens to several hundreds of years could represent ephemeral events within the time period that a given sampling depth represents. This interpretation implies persistent high frequency (centennial to decadal) and high amplitude (>5000 yr) variability in the ventilation age of Nordic Seas overflows during the last deglaciation. Alternatively, the ages given by *Pyrgo* species may simply be too old. This enigma represents a critical obstacle to make robust inferences about ocean circulation changes and North Atlantic-Arctic Mediterranean deep-water exchanges in the light of bottom water ^{14}C ventilation-age reconstructions. It is therefore crucial to investigate the reliability of the radiocarbon dates measured in *Pyrgo* species from the glacial and deglacial sediments from the Arctic Mediterranean and the subpolar North Atlantic Ocean.

A key observation in the study of Thornalley et al. (2015) is the abrupt aging of deep water in the northern Norwegian Seas to 7640 ^{14}C years (with B-P age of 6210 ^{14}C years) at ~22 ka (at uncalibrated planktic ^{14}C date of 19,790 yr before present (BP)). The authors suggested that pre-aged water from the central Arctic Ocean flowed into the Norwegian Sea through the Fram Strait during the LGM. Sediments dating from the LGM from the Fram Strait should therefore record the hypothesized outflow of 'extremely aged' Arctic deep water. However, our LGM B-P age differences from the Fram Strait do not support an outflow from the Arctic Ocean with >6000 ^{14}C years old water to the Nordic Seas (Fig. 4e, Table 1). These contrasting results are most likely due to the use of *Pyrgo* for ^{14}C measurements in previous reconstructions (Ezat et al., 2017). It is important to note that the LGM sediments in our records from the Fram Strait do not contain any *Pyrgo* species and radiocarbon dates could only be obtained on *O. umbonatus* (the only abundant calcareous benthic foraminifer; Supplementary Fig. 1). There is a small peak in the abundance of *Pyrgo* species in core HH12-946MC during late MIS 3 (33.5–26 ka), and their radiocarbon dates are 6000–8000 yr older than the dates performed in *O. umbonatus* (Supplementary Fig. 1; Table 1). While the $\delta^{13}C$ of *P. depressa* and *O. umbonatus* are very similar in the Holocene interval, the $\delta^{13}C$ of *P. depressa* are significantly higher in MIS 3 (Table 1, Supplementary Table 1). This relative increase in $\delta^{13}C$ of *P. depressa* is, at face value, inconsistent with the idea that *P. depressa* records an older water mass than *O. umbonatus*.

To explore further the reliability of *Pyrgo* ^{14}C dates, two new radiocarbon dates were measured in *N. pachyderma* and *Pyrgo rotalaria* specimens from one glacial sample from the southern Norwegian Sea (core LINK15; Fig. 1). The uncalibrated radiocarbon ages of *N. pachyderma* and *Pyrgo rotalaria* are 21,750 and 29,395 ^{14}C years BP, respectively, with a B-P age difference of 7642 ^{14}C years. This age difference of 7642 ^{14}C years between *P. rotalaria* and *N. pachyderma* from the southern Norwegian Sea also cannot be explained

by an aged outflow from the Arctic/northern Norwegian Sea, because the previously suggested 'extreme aging' in the northern Norwegian Sea started later (at uncalibrated planktic ^{14}C date of 19,790 ^{14}C years BP; Thornalley et al., 2015; see above). We would expect that the signature of the extremely aged water to appear earlier or nearly at the same time in the northern Norwegian Sea compared to the southern Norwegian Sea to be consistent with the scenario proposed by Thornalley et al. (2015). Thus, this result support the evidence that the older ^{14}C dates measured in *Pyrgo* species compared to other species in the samples are not a result of recording bottom-water radiocarbon activity.

A remaining question is what did cause the too old *Pyrgo* ^{14}C dates? Magana et al. (2010) proposed that similarly old *Pyrgo* ages from deglacial sediments from the Santa Barbara Basin in the eastern Pacific Ocean were caused by presence of radiocarbon-free hydrocarbons in the calcifying environment. This was based on the associated low *Pyrgo* δ^{13}C (−4 to −8‰). In contrast, the old *Pyrgo* ^{14}C ages from the Nordic Seas are associated with high δ^{13}C of 0.6 to 1.1‰, which are ∼1.5 ‰ higher than δ^{13}C of coeval infaunal benthic species of much younger ^{14}C ages (Table 1, see also Thornalley et al., 2015; Ezat et al., 2017). At 332 m water depth off Northern Norway, samples of deglacial age dated on *Quinqueloculina* sp. and mixed miliolid species yielded ^{14}C ages that are up to 5000 yr older than their stratigraphic chronology and coeval bivalve shells (Vorren and Plassen, 2002). In Holocene shelf sediments from Skaw Spit, Denmark, mixed miliolid species also gave up to 5000 yr older ages than coeval other benthic foraminifera and bivalve shells (Heier-Nielsen et al., 1995). This was here interpreted as miliolids had been laterally transported from older sediments. Lateral or downslope reworking of older fossil *Pyrgo* specimens seem also a plausible explanation for the too old ages recorded for some time intervals in the Nordic Seas and the subpolar North Atlantic (Ezat et al., 2017 and references therein). Indeed, Vorren and Plassen (2002) and Heier-Nielsen et al. (1995) studies suggest that ^{14}C dating of miliolid species other than *Pyrgo* species may also be questionable, but this requires additional investigation. Ezat et al. (2017) speculated that the too old ages of *Pyrgo* species in the glacial Arctic Mediterranean might have resulted from unknown 'vital effects' adopted by *Pyrgo* species under specific environmental conditions. For example, microbial fermentation (e.g., by endosymbiotic microbes) of old organic matter, which may have been more readily available during glacial ice-rafting and/or meltwater discharge events, will result in high δ^{13}C and ^{14}C-depleted bicarbonate (see Carothers and Kharaka, 1980). However, *Pyrgo* species from deglacial and glacial sediments do not always date too old. For example, *Pyrgo* dates from the central Nordic Seas at ∼28–23 ka and ∼16.5 ka give ventilation ages <2000 yr (Thornalley et al., 2015). We are thus not able to specify the exact mechanisms responsible for the old *Pyrgo* ^{14}C ages (indeed, different mechanisms might prevail in different contexts), however we can confirm that an Arctic deep outflow of >6000 yr old water to the Nordic Seas during the LGM (26–20 ka) could not be traced to its putative source in our Fram Strait records.

3.3. Implications for the LGM climate

Bottom water temperature reconstructions from the Faroe-Shetland Channel at 1200 m water depth from the southern Norwegian Sea show persistently high bottom water temperature (∼3°C higher than modern) at 26–20 ka comprising the LGM (Ezat et al., 2014). This increase in bottom water temperature has been explained by inflow of warm Atlantic water below a buoyant layer (Ezat et al., 2014) as previously suggested for glacial stadial periods (e.g., Rasmussen and Thomsen, 2004). Upwelling of deep water in the Fram Strait and probably in other areas in the northern Nordic Seas provides an outflow pathway that may be necessary to main-

tain the subsurface inflow of Atlantic water into the Nordic Seas. This subsurface northward inflow of Atlantic water and subsequent upwelling during the LGM may have provided a source of local moisture for the Svalbard-Barents Sea Ice sheet (e.g., Hebbeln et al., 1994), which continued to grow until 21 ka (e.g., Hughes et al., 2016). This is in agreement with biomarker studies from the Fram Strait and the eastern Yermark Plateau that show mainly seasonal sea-ice during the LGM and not a permanent sea-ice cover (Müller and Stein, 2014; see Fig. 4b, c). The increase in primary productivity due to upwelling of nutrient-rich water may have enhanced photosynthetic removal of CO_2 from the surface ocean enhancing local oceanic CO_2 uptake from the atmosphere. However, a more direct proxy for surface ocean pCO_2 would be needed to confirm this, as the pCO_2 drawdown via increased primary productivity may have been balanced or exceeded by the effects of higher total dissolved CO_2 in the upwelled deep water.

Furthermore, our finding that the Arctic Ocean was not extremely aged during the late glacial has important implications for the interpretation of ocean circulation changes in the North Atlantic. For example, Keigwin and Swift (2017) found indications of presence of a relatively young and nutrient-depleted water mass during the LGM (21–18 ka) at 5000 m water depth in the subtropical western North Atlantic. The authors of this study excluded the Arctic Mediterranean to be the source of this water mass because of previous inferences of an extremely aged (and thus likely isolated) deep Arctic Mediterranean (Thornalley et al., 2015). Instead, they suggested the Labrador Sea as the most likely source. With our new results, the Arctic Mediterranean should not be ruled out as a possible source of this deep-water mass in the Western North Atlantic. In principle, water mass source proxies (e.g., Nd isotopes) from both regions could potentially reveal the source of the 5000 m deep water mass found in the western North Atlantic during the LGM.

Finally, the close timing between the decrease in atmospheric radiocarbon content ∼26–20 ka (e.g., Reimer et al., 2013) and our 'inferred' upwelling of aged (∼2000 yr old) deep water in the Fram Strait (and probably in other areas in the Nordic Seas) suggests a possible non-negligible impact on the (radio-)carbon cycle via the high northern latitudes. These findings therefore encourage additional work to further explore the spatial extent of upwelling and/or deep mixing in the Nordic Seas, and to assess the impacts on ocean-atmosphere exchanges of heat and carbon.

4. Conclusions

In this study, we have reconstructed deep ocean circulation changes in the central Fram Strait in two records from >2500 m water depth, using ^{14}C dates on benthic and planktic foraminiferal species alongside multispecies carbon and oxygen stable isotope measurements. We show that the hypothesized model of Arctic purging of extremely aged deep water (>6000 yr old water) into the Nordic Seas during the LGM and to the subpolar North Atlantic during the last deglaciation is likely biased due to the use of *Pyrgo* species for dating. Our ventilation age estimates show significant aging (∼2000 yr old water) and strong stratification during late MIS 3 in the Fram Strait suggesting a dramatic reduction/shoaling of deep-water formation in the Arctic Mediterranean. During the LGM, ocean stratification broke down due to enhanced vertical mixing, which resulted in an increase in primary productivity. We show that the physical oceanographic and biological state in the Fram Strait and northern Nordic Seas during the period 26–21 ka could have contributed to the final intensification phase of the last glacial via local ocean-atmosphere exchange of heat, moisture and carbon, thus underlining the climatic importance of positive feedbacks between the atmosphere, ocean circulation, carbon cycle, and cryosphere in high northern latitudes.

Competing financial interests

The authors declare no competing financial interests.

Acknowledgements

Appendix A. Supplementary material

Supplementary material related to this article can be found online at https://doi.org/10.1016/j.epsl.2019.04.027.

References

Aagaard, K., Swift, J.H., Carmack, E.C., 1985. Thermohaline circulation in the Arctic Mediterranean seas. J. Geophys. Res., Oceans 90, 4833–4846.

Adkins, J.F., Boyle, E.A., 1997. Changing atmospheric Δ^{14}C and the record of deep water paleoventilation ages. Paleoceanography 12, 337–344.

Bard, E., 1988. Correction of accelerator mass spectrometry ^{14}C ages measured in planktonic foraminifera: paleoceanographic implications. Paleoceanography 3, 635–645.

Bauch, H.A., Erlenkeuser, H., Spielhagen, R.F., Struck, U., Matthiessen, J., Thiede, J., Heinemeier, J., 2001. A multiproxy reconstruction of the evolution of deep and surface waters in the subarctic Nordic seas over the last 30,000 yr. Quat. Sci. Rev. 20, 659–678.

Broecker, W.S., Peng, T.H., 1982. Tracers in the Sea. Eldigio Press, Palisades, New York.

Broecker, W., Barker, S., Clark, E., Hajdas, I., Bonani, G., Stott, L., 2004. Ventilation of the glacial deep Pacific Ocean. Science 306, 1169–1172.

Carothers, W.W., Kharaka, Y.K., 1980. Stable carbon isotopes of HCO_3^- in oil-field waters—implications for the origin of CO_2. Geochim. Cosmochim. Acta 44, 323–332.

Clark, P.U., Pisias, N.G., Stocker, T.F., Weaver, A.J., 2002. The role of the thermohaline circulation in abrupt climate change. Nature 415, 863.

Clark, P.U., Dyke, A.S., Shakun, J.D., Carlson, A.E., Clark, J., Wohlfarth, B., Mitrovica, J.X., Hostetler, S.W., McCabe, A.M., 2009. The last glacial maximum. Science 325, 710–714.

Cook, M.S., Keigwin, L.D., 2015. Radiocarbon profiles of the NW Pacific from the LGM and deglaciation: evaluating ventilation metrics and the effect of uncertain surface reservoir ages. Paleoceanography 30, 174–195.

Curry, W.B., Oppo, D.W., 2005. Glacial water mass geometry and the distribution of δ^{13}C of ΣCO_2 in the western Atlantic Ocean. Paleoceanography 20.

Dokken, T.M., Hald, M., 1996. Rapid climatic shifts during isotope stages 2–4 in the Polar North Atlantic. Geology 24, 599–602.

Ezat, M.M., Rasmussen, T.L., Groeneveld, J., 2014. Persistent intermediate water warming during cold stadials in the southeastern Nordic seas during the past 65 ky. Geology 42, 663–666.

Ezat, M.M., Rasmussen, T.L., Thornalley, D.J., Olsen, J., Skinner, L.C., Hönisch, B., Groeneveld, J., 2017. Ventilation history of Nordic Seas overflows during the last (de)glacial period revealed by species-specific benthic foraminiferal ^{14}C dates. Paleoceanography 32, 72–181.

Freeman, E., Skinner, L.C., Reimer, R., Scrivner, A.E., Fallon, S., 2015. Graphitization of small carbonate samples for palaeoceanographic research at the Godwin Radiocarbon Laboratory, University of Cambridge. Radiocarbon 58, 89–97.

Ganachaud, A., Wunsch, C., 2000. Improved estimates of global ocean circulation, heat transport and mixing from hydrographic data. Nature 408, 453.

Gottschalk, J., Szidat, S., Michel, E., Mazaud, A., Salazar, G., Battaglia, M., Lippold, J., Jaccard, S.L., 2018. Radiocarbon measurements of small-size foraminiferal samples with the Mini Carbon Dating System (MICADAS) at the University of Bern: implications for paleoclimate reconstructions. Radiocarbon 60, 469–491.

Hansen, B., Østerhus, S., 2000. North Atlantic–Nordic seas exchanges. Prog. Oceanogr. 45, 109–208.

Hanslik, D., Jakobsson, M., Backman, J., Björck, S., Sellén, E., O'Regan, M., Fornaciari, E., Skog, G., 2010. Quaternary Arctic Ocean sea ice variations and radiocarbon reservoir age corrections. Quat. Sci. Rev. 29, 3430–3441.

Hebbeln, D., Dokken, T., Andersen, E.S., Hald, M., Elverhøi, A., 1994. Moisture supply for northern ice-sheet growth during the Last Glacial Maximum. Nature 370, 357.

Heier-Nielsen, S., Conradsen, K., Heinemeier, J., Knudsen, K.L., Nielsen, H.L., Rud, N., Sveinbjörnsdóttir, Á.E., 1995. Radiocarbon dating of shells and foraminifera from the Skagen core, Denmark: evidence of reworking. Radiocarbon 37, 119–130.

Hoffmann, S.S., McManus, J.F., Curry, W.B., Brown-Leger, L.S., 2013. Persistent export of ^{231}Pa from the deep central Arctic Ocean over the past 35,000 years. Nature 497, 603–606.

Hughes, A.L., Gyllencreutz, R., Lohne, Ø.S., Mangerud, J., Svendsen, J.I., 2016. The last Eurasian ice sheets – a chronological database and time-slice reconstruction, DATED-1. Boreas 45, 1–45.

Keigwin, L.D., 1979. Late Cenozoic stable isotope stratigraphy and paleoceanography of DSDP sites from the east equatorial and central North Pacific Ocean. Earth Planet. Sci. Lett. 45, 361–382.

Keigwin, L.D., Swift, S.A., 2017. Carbon isotope evidence for a northern source of deep water in the glacial western North Atlantic. Proc. Natl. Acad. Sci. 114, 2831–2835.

Kroopnick, P.M., 1985. The distribution of ^{13}C of ΣCO_2 in the world oceans. Deep-Sea Res., A, Oceanogr. Res. Pap. 32, 57–84.

Magana, A.L., Southon, J.R., Kennett, J.P., Roark, E.B., Sarnthein, M., Stott, L.D., 2010. Resolving the cause of large differences between deglacial benthic foraminifera radiocarbon measurements in Santa Barbara Basin. Paleoceanography 25, PA4102.

Mangerud, J., Bondevik, S., Gulliksen, S., Hufthammer, A.K., Høisæter, T., 2006. Marine ^{14}C reservoir ages for 19th century whales and molluscs from the North Atlantic. Quat. Sci. Rev. 25, 3228–3245.

Meinhardt, A.K., Pahnke, K., Böning, P., Schnetger, B., Brumsack, H.J., 2016. Climate change and response in bottom water circulation and sediment provenance in the Central Arctic Ocean since the Last Glacial. Chem. Geol. 427, 98–108.

Müller, J., Stein, R., 2014. High-resolution record of late glacial and deglacial sea ice changes in Fram Strait corroborates ice–ocean interactions during abrupt climate shifts. Earth Planet. Sci. Lett. 403, 446–455.

Olsen, J., Rasmussen, T.L., Reimer, P.J., 2014. North Atlantic marine radiocarbon reservoir ages through Heinrich event H4: a new method for marine age model construction. Geol. Soc. (Lond.) Spec. Publ. 398, 95–112.

Otto-Bliesner, B.L., Hewitt, C., Marchitto, T., Brady, E., Abe-Ouchi, A., Crucifix, M., Murakami, S., Weber, S., 2007. Last Glacial Maximum ocean thermohaline circulation: PMIP2 model intercomparisons and data constraints. Geophys. Res. Lett. 34, L12706.

Pados, T., Spielhagen, R.F., Bauch, D., Meyer, H., Segl, M., 2015. Oxygen and carbon isotope composition of modern planktic foraminifera and near-surface waters in the Fram Strait (Arctic Ocean) – a case study. Biogeosciences 12, 1733–1752.

Pena, L.D., Goldstein, S.L., 2014. Thermohaline circulation crisis and impacts during the mid-Pleistocene transition. Science 345, 318–322.

Peng, T-H., Broecker, W., 1984. The impacts of bioturbation on the age difference between benthic and planktonic foraminifera in deep sea sediments. Nucl. Instrum. Methods Phys. Res. 5, 346–352.

Rahmstorf, S., 2000. The thermohaline ocean circulation: a system with dangerous thresholds? Clim. Change 46, 247–256.

Rasmussen, T.L., Thomsen, E., 2004. The role of the North Atlantic Drift in the millennial timescale glacial climate fluctuations. Palaeogeogr. Palaeoclimatol. Palaeoecol. 210, 101–116.

Reimer, P.J., Bard, E., Bayliss, A., Beck, J.W., Blackwell, P.G., Ramsey, C.B., Buck, C.E., Cheng, H., Edwards, R.L., Friedrich, M., Grootes, P.M., 2013. IntCal13 and Marine13 radiocarbon age calibration curves 0–50,000 years cal BP. Radiocarbon 55, 1869–1887.

Sarnthein, M., Winn, K., Jung, S.J., Duplessy, J.C., Labeyrie, L., Erlenkeuser, H., Ganssen, G., 1994. Changes in east Atlantic deepwater circulation over the last 30,000 years: eight time slice reconstructions. Paleoceanography 9, 209–267.

Skinner, L.C., Fallon, S., Waelbroeck, C., Michel, E., Barker, S., 2010. Ventilation of the deep Southern Ocean and deglacial CO_2 rise. Science 328, 1147–1151.

Skinner, L.C., Waelbroeck, C., Scrivner, A.E., Fallon, S.J., 2014. Radiocarbon evidence for alternating northern and southern sources of ventilation of the deep Atlantic carbon pool during the last deglaciation. Proc. Natl. Acad. Sci. 111, 5480–5484.

Stuiver, M., Reimer, P.J., 1993. Extended ^{14}C data base and revised CALIB 3.0 ^{14}C age calibration program. Radiocarbon 35, 215–230.

Takahashi, T., Sutherland, S.C., Wanninkhof, R., Sweeney, C., Feely, R.A., Chipman, D.W., Hales, B., Friederich, G., Chavez, F., Sabine, C., Watson, A., 2009. Climatological mean and decadal change in surface ocean pCO$_2$, and net sea–air CO_2

flux over the global oceans. Deep-Sea Res., Part 2, Top. Stud. Oceanogr. 56, 554–577.

Thornalley, D.J.R., Barker, S., Broecker, W.S., Elderfield, H., McCave, I.N., 2011. The deglacial evolution of North Atlantic deep convection. Science 331, 202–205.

Thornalley, D.J.R., Bauch, H.A., Gebbie, G., Guo, W., Ziegler, M., Bernasconi, S.M., Barker, S., Skinner, L.C., Yu, J., 2015. A warm and poorly ventilated deep Arctic Mediterranean during the last glacial period. Science 349, 706–710.

Veum, T., Jansen, E., Arnold, M., Beyer, I., Duplessy, J.C., 1992. Water mass exchange between the North Atlantic and the Norwegian Sea during the past 28,000 years. Nature 356, 783.

Vorren, T.O., Plassen, L.I.V., 2002. Deglaciation and palaeoclimate of the Andfjord-Vågsfjord area, North Norway. Boreas 31, 97–125.

Zamelczyk, K., Rasmussen, T.L., Husum, K., Haflidason, H., de Vernal, A., Ravna, E.K., Hald, M., Hillaire-Marcel, C., 2012. Paleoceanographic changes and calcium carbonate dissolution in the central Fram Strait during the last 20 ka. Quat. Res. 78, 405–416.

Zamelczyk, K., Rasmussen, T.L., Husum, K., Godtliebsen, F., Hald, M., 2014. Surface water conditions and calcium carbonate preservation in the Fram Strait during marine isotope stage 2, 28.8–15.4 kyr. Paleoceanography 29, 1–12.

Zamelczyk, K., Rasmussen, T.L., Groeneveld, J., Raitzsch, M., 2016. Paleoceanographic changes and near sea surface temperatures (SST) in the western-central Fram Strait over the last 47 kyr. In: ICP 2016, Poster Session 2: Paleo Proxies: Development, Calibration and Application, P-291. Utrecht, Netherlands.